

# Gene Expression and Growth Factor Analysis in Early Nerve Regeneration following Segmental Nerve Defect Reconstruction with a Mesenchymal Stromal Cell-enhanced Decellularized Nerve Allograft

Nadia Rbia, MD\*†  
 Liselotte F. Bulstra, PhD\*†  
 Patricia F. Friedrich, AAS\*  
 Allen T. Bishop, MD\*  
 Tim H.J. Nijhuis, MD, PhD†  
 Alexander Y. Shin, MD\*

**Background:** The purpose of this study was to evaluate the molecular mechanisms underlying nerve repair by a decellularized nerve allograft seeded with adipose-derived mesenchymal stromal cells (MSCs) and compare it to the unseeded allograft and autograft nerve.

**Methods:** Undifferentiated MSCs were seeded onto decellularized nerve allografts and used to reconstruct a 10 mm gap in a rat sciatic nerve model. Gene expression profiles of genes essential for nerve regeneration and immunohistochemical staining (IHC) for PGP9.5, NGF, RECA-1, and S100 were obtained 2 weeks postoperatively.

**Results:** Semi-quantitative RT-PCR analysis showed that the angiogenic molecule *VEGFA* was significantly increased in seeded allografts, and transcription factor *SOX2* was downregulated in seeded allografts. Seeded grafts showed a significant increase in immunohistochemical markers NGF and RECA-1, when compared with unseeded allografts.

**Conclusions:** MSCs contributed to the secretion of trophic factors. A beneficial effect of the MSCs on angiogenesis was found when compared with the unseeded nerve allograft, but implanted MSCs did not show evidence of differentiation into Schwann cell-like cells. (*Plast Reconstr Surg Glob Open* 2020;8:e2579; doi: 10.1097/GOX.0000000000002579; Published online 21 January 2020.)

## INTRODUCTION

Nerve graft substitutes remain inferior to autografts for the repair of motor and mixed peripheral nerve injuries.<sup>1</sup> Nerve regeneration is a complicated process highlighted by Wallerian degeneration, axonal sprouting, and myelination.<sup>2</sup> In response to injury, Schwann cells (SCs) produce high levels of neurotrophic growth factors.<sup>3</sup> Successful crossing of a nerve gap depends on the formation of a new extracellular matrix (ECM) scaffold, over which blood vessels, fibroblasts, and SCs can migrate and regenerate

towards the distal nerve stump.<sup>4</sup> Acellular nerve grafts are rich in ECM components; however, they lack viable SCs.<sup>5</sup> Supplementing acellular nerve grafts with supporting cells may improve outcomes.<sup>6</sup>

Previously, researchers have successfully supplemented acellular nerve grafts with cultured SCs.<sup>7,8</sup> However, efficiently obtaining autologous SCs for clinical use is difficult as it requires harvest of a donor nerve and time to culture and proliferate.<sup>6</sup> Adipose-derived mesenchymal stromal cells (MSCs) are easily accessible, rapidly expandable, capable of survival/integration within the host tissue and can be guided into non-mesenchymal lineages, such as neurons, astrocytes, and SC-like cells to support nerve regeneration.<sup>2,9</sup> *In vitro* differentiation is a time-consuming process and limits clinical applicability. Thus, application of undifferentiated MSCs,

From the \*Department of Orthopedic Surgery, Mayo Clinic, Rochester, Minn.; and †Department of Plastic, Reconstructive and Hand Surgery, Erasmus Medical Center, Rotterdam, The Netherlands.

Received for publication June 12, 2019; accepted October 21, 2019.

Part of this work was presented at the Annual Meeting of the American Society for Peripheral Nerve, January 13, 2017, Waikoloa, Hawaii.

Copyright © 2020 The Authors. Published by Wolters Kluwer Health, Inc. on behalf of The American Society of Plastic Surgeons. This is an open-access article distributed under the terms of the [Creative Commons Attribution-Non Commercial-No Derivatives License 4.0 \(CCBY-NC-ND\)](#), where it is permissible to download and share the work provided it is properly cited. The work cannot be changed in any way or used commercially without permission from the journal.

DOI: 10.1097/GOX.0000000000002579

**Disclosure:** Research reported in this publication was supported by the National Institute of Neurological Disorders and Stroke of the National Institutes of Health under Award Number R01NS102360. The content is solely the responsibility of the authors and does not necessarily represent the official views of the National Institutes of Health.

Related Digital Media are available in the full-text version of the article on [www.PRSGlobalOpen.com](http://www.PRSGlobalOpen.com).

which have been recently shown to improve nerve conduction velocity,<sup>10</sup> is an attractive alternative.

Evaluations of nerve regeneration have relied heavily on functional evaluations. Although these approaches have the potential to be clinically relevant, they do not provide insight into the mechanisms underlying the neurotrophic potential of MSCs.<sup>11</sup> Despite the popular theory that release of growth factors is a potential mechanism of the cells' restorative capacity, quantitative analysis of neurotrophic factor release from implanted MSCs is rarely reported<sup>12</sup> (see figure, Supplemental Digital Content 1, which displays the proposed mechanism of how cell-based therapy can create a more favorable environment for peripheral nerve regeneration is depicted, <http://links.lww.com/PRSGO/B268>).

Questions regarding cell fate and differentiation remain unanswered. The purpose of this study was to evaluate the molecular mechanisms underlying nerve repair with a decellularized nerve allograft seeded with isogenic, undifferentiated, adipose-derived MSCs.

## MATERIALS AND METHODS

After IACUC institutional review committee approval, isogenic Lewis rat MSCs were dynamically seeded onto Sprague Dawley rat decellularized nerve allografts (N = 9) and used to bridge a 10-mm sciatic nerve defect in Lewis rats. Sprague-Dawley rats were chosen as nerve donors, as there is a major histocompatibility mismatch to the recipient Lewis rat.<sup>13</sup> This mismatch would mimic the human clinical situation. The fate of implanted MSCs was determined by evaluating gene expression profiles 2 weeks postoperatively. IHC staining was obtained for neurite outgrowth, angiogenesis, and SCs to determine whether up or downregulation of growth factor levels had functional consequences for early nerve regeneration. Outcomes were compared with unseeded allografts (N = 9) and autograft controls (N = 9).

### Isolation of Rat MSCs

MSCs were obtained from the inguinal fat pad of inbred Lewis rats, as previously described by Kingham et al.<sup>14</sup> Cultures were maintained at subconfluent levels in a 37°C incubator with 5% CO<sub>2</sub> and passaged with TrypLE (Invitrogen). MSCs were then lentivirally transduced to express the firefly luciferase, as previously described.<sup>15</sup> This method has been shown to display no differences in viability and cell proliferation between labeled/unlabeled cells and luciferase was expressed steadily in vitro. All MSCs used in the experiment were of passage 5 and have previously been shown to be capable of multilineage differentiation.<sup>15</sup> Undifferentiated MSCs were used as they have been shown respond to the demands placed on them by the local environment.

### Preparation of Allografts

A total of 18 rat sciatic nerve segments of 1.5 cm were harvested from Sprague-Dawley rats, weighing 250–350 g (Harlan, Indianapolis, Ind.). Sciatic nerves were aseptically excised, cleared of peripheral fat tissue, and decellularized using the protocol utilizing elastase as previously described.<sup>16</sup> Before surgery, 9 decellularized allografts were dynamically seeded with passage 5 Lewis rat MSCs as

previously described.<sup>17</sup> Nerve allografts were combined with MSCs in a 15-ml TubeSpin Bioreactor tube containing 10-ml cell culture medium and 1 million cells per nerve. After 12 hours of incubation, seeded nerves were used for surgery.

### Surgical Procedure

Lewis rats (N = 27) weighing 250–350 g (Harlan) were anesthetized and surgical procedures were performed under standard aseptic conditions, as previously described by Hundepool et al.<sup>18</sup> All allografts were cut to 10 mm. In group I, seeded allografts (N = 9) were used to bridge the 10-mm nerve gap using 10-0 nylon epineural sutures (Ethicon, Inc., Somerville, N.J.). In group II, acellular allografts (N = 9) were used. In the control group III, autologous nerve segments were reversed and sutured back.

### Outcome Measurements

Two weeks postoperatively, anesthesia was induced using isoflurane and all animals (N = 27) were sacrificed with an intraperitoneal overdose of Fatal-Plus (Vortech Pharmaceuticals, Dearborn, Mich.).

### Quantitative Real-time Reverse-transcriptase Polymerase Chain Reaction

Changes in relative gene expression profiles of MSCs seeded allografts were evaluated by quantitative real-time reverse-transcriptase polymerase chain reaction and compared with unseeded allografts and autograft controls (N = 5 per group). Nerve segments were harvested, frozen in QIAzol Lysis Reagent (Qiagen, Valencia, Calif.) and stored at –80°C. Total RNA was extracted using the miRNeasy Mini Kit (Qiagen) and RNA yield was evaluated using a Nanodrop 2000 (Thermo Scientific, Inc., Waltham, Mass.) followed by reverse transcription into cDNA by RT-PCR using SuperScript III (Invitrogen). Resulting cDNA libraries were analyzed by quantitative real-time reverse-transcriptase polymerase chain reaction (C1000 Touch Thermalk Cycler, BioRad, Hercules, Calif.) using SYBR Green detection with specific primers, chosen from the literature, for a panel of genes essential for nerve regeneration (Table 1). Results were analyzed to map MSC characteristics including proliferation, apoptosis, myelination, and ECM-production.<sup>8,19,21</sup> Samples were analyzed in triplicate and results were normalized to the reference housekeeping gene GAPDH within each sample and then normalized to the unseeded allograft group. Differences in gene expression levels were quantified using the comparative delta crossover threshold [ $2^{(-\Delta\Delta Ct)}$ ] method.<sup>22</sup>

### Immunohistochemical Staining

Sciatic nerves (N = 4) of the operated sites were explanted over a length from 5 mm proximal and distal to the graft, fixed in 4% Paraformaldehyde (Sigma), suspended in Tissue-Tek OCT Compound, and snap frozen. Transverse sections (5-μm thick) were cut on a cryostat at different levels within the middle of the repair site (see figure, Supplemental Digital Content 2, which displays transverse sections were cut on a cryostat at different levels within the middle of the nerve, <http://links.lww.com/PRSGO/B269>).

**Table 1. mRNA Primer Sequences**

Gene ID	Biology	Forward Primer	Reverse Primer
GAPDH	Reference gene	TACCAGGGCTGCCTTCTCTTG	GGATCTCGCTCCTGGAAGATG
NGF	Neurotrophic marker	CACCTCTGAGGTGCATAGCGT	CTATTGGTTACGACGGGGCA
GDNF	Neurotrophic marker	CGCTGACCAGTGACTCCAATA	GCGACCTTTCCTCTGGAAT
PTN	Neurotrophic marker	GCCGAGTGCAAACAACCAT	TGATTCCGCTTGAGGCTTGG
GAP43	Cytoplasmic protein	GATAACTCGCCGTCCCTCAA	CTACAGCTTCTTCTCCTCCTCA
VEGFA	Angiogenic marker	CAGAAAGCCCATGAAGTGGTG	CTTCATCATTCGACGAGCCC
PECAM1/CD31	Angiogenic marker	TTGTGACCAGTCTCCGAAGC	TGGCTGTTGGTTTCCACACT
MPZ	Myelination marker	AGGCCGAGATGCCATTTCAA	CCCATACCTAGTGGGCACTTT
PMP22	Myelination marker	GTCTGGTCTGCTGTGAGCAT	GCCATTGGCTGACGATGGTG
MBP	Myelination marker	TCTGGCAAGGACTCACACAC	AAATCTGCTGAGGGACAGGC
COL1A1	ECM protein	AAGTCTCAAGATGGTGGCCG	TCGATCCAGTACTCTCCGCT
COL3A1	ECM protein	CCCGCAACAATGGTAATCC	GACCTCGTGCTCCAGTTAGC
LAMB2	ECM protein	AGTACCCACACGGATGGAGTG	CTCGAGAACAGCCAGGTACA
FBLN1	ECM protein	CGAGACACCTTTCGCCAAGA	CGTGACAGCCCTCAGAAAGA
CASP3	Apoptosis protein	GGAGCTTGGAACGCCAAGAA	ACACAAGCCCATTTCAGGGT
EGR1	Transcription factor	CACCTGACCACAGAGTCCTTTT	GTTGGAGGGTTGGTTCATGCT
SOX2	Transcription factor	AGTGGTACGTTAGGCGCTTC	CCCACAGAACCCTTTTCCT
CCNB2	Protein coding gene	ACCAGTGCAGATGGAGACAC	GACTGCAAAGCCTCAAGCTG
FABP4	Protein coding gene	TGAAAGAAGTGGGAGTTGGCTT	TGGTGCAGTTTCCATCCCAC

Sequences for primers used in qPCR reactions (ECM). The following genes were analyzed: glyceraldehyde 3-phosphate dehydrogenase (GAPDH), nerve growth factor (NGF), glial cell line-derived neurotrophic factor (GDNF), pleiotrophin (PTN), growth associated protein 43 (GAP43), vascular endothelial cell growth factor alpha (VEGFA), platelet endothelial cell adhesion molecule 1 (PECAM1/CD31), myelin protein zero (MPZ), peripheral myelin protein 22 (PMP22), myelin basic protein (MBP), collagen type 1 (COL1A1) and 3 (COL3A1), laminin subunit beta 2 (LAMB2), fibulin 1 (FBLN1), caspase 3 (CASP3), early growth response protein (EGR1), sex determining region y-box 2 (SOX2), cyclin B2 (CCNB2), and fatty acid binding protein 4 (FABP4).

IHC staining was obtained for PGP9.5, NGF, RECA-1, and S100. Luciferase labeled MSCs were also double stained for Luciferase and S100 to study MSC differentiation to SC like cells. Slides were stored at  $-80^{\circ}\text{C}$  and before staining dried for 2 hours. Slides were manually post fixed and retrieved online using Epitope Retrieval 1 (Leica Microsystems). Sections were incubated for 60 minutes at  $24^{\circ}\text{C}$  in the following primary antibodies: polyclonal S100 anti-rabbit (Dako Z0311) was used at 1:5,000; polyclonal PGP9.5 anti-rabbit (Dako Z5116) was used at 1:500; monoclonal RECA-1 anti-mouse (Abcam ab9774) was used at 1:200; monoclonal NGF anti-rabbit (Abcam ab52918) was used at 1:150 and polyclonal anti-rabbit Firefly Luciferase (Abcam ab21176) was used at 1:2,000. Sections were then washed with PBS and incubated with secondary antibodies [Alexa Fluor 568 or 488 Goat-anti-Rabbit (Invitrogen) at  $24^{\circ}\text{C}$  for 60 minutes]. The Research Detection System (Leica DS9455) was used and included Rodent Block R (Biocare RBR962). Cell nuclei were stained with Hoechst 33342 (Invitrogen H1399). Once completed, slides were rinsed in distilled water, coverslipped, and observed by a confocal microscope (LSM 780, Zeiss). Nerve areas were captured at  $\times 10$  (tile-scan) and  $\times 20$  magnification.

### Image Analysis

Fluorescence intensity in the nerve cross-sections was measured using ImageJ (NIH, Bethesda, MD) to quantify differences between the grafts. All images were obtained with the same settings and analysis was performed on the antibody monolayer, without Hoechst. A representative area was selected and the integrated density was measured. To determine and correct for the background signal, 3 areas of the image that had no fluorescence were selected and mean gray value was measured. Results were used to calculate the corrected total cell fluorescence (CTCF).<sup>23</sup>

### Statistical Analysis

The Kolmogorov-Smirnoff test was applied to test for a normal distribution. To detect differences between groups,

data were analyzed using the Kruskal-Wallis test followed by the Dunn-Bonferroni post hoc test. Statistically significance was set at  $P < 0.05$ . All results are reported as mean  $\pm$  SD.

## RESULTS

### Quantitative Real-time Reverse-transcriptase Polymerase Chain Reaction

All animals survived and there were no surgical complications. Supplemental Figure 3a–d demonstrates the expression levels clustered by genes sharing a common function. *NGF*, *GDNF*, *PTN*, and *GAP43* were chosen as representative neurotrophic factors as they have been shown to promote neuronal survival and axonal regeneration after peripheral nerve injury<sup>11</sup> [see figure, Supplemental Digital Content 3, which displays relative gene expression 14 days postoperatively. A, *NGF*, *GDNF*, *PTN*, and *GAP43* mRNA expression levels were measured in the autograft, allograft, and MSC seeded nerve allograft ( $n = 5$ ). Relative expression levels are shown with regard to the allograft (value = 1)  $*P < 0.05$ . B, *VEGFA*, *CD31*, *MPZ*, *PMP22*, and *MBP* mRNA expression levels were measured. Relative expression levels are shown with regard to the allograft (value = 1)  $*P < 0.05$ . C, *COL1A1*, *COL3A1*, *LAMB2*, and *FBLN1* mRNA expression levels were measured. Relative expression levels are shown with regard to the allograft (value = 1). D, *CASP3*, *EGR1*, *SOX2*, *CCNB2*, and *FABP4* mRNA expression levels were measured. Relative expression levels are shown with regard to the allograft (value = 1), <http://links.lww.com/PRSGO/B270>].

Analysis showed significantly higher *NGF* mRNA levels after autograft reconstruction when compared with the unseeded allograft (2.3-fold increase,  $P = 0.047$ ) or the seeded nerve allograft (2.6-fold increase  $P = 0.038$ ). There was no significant difference between the allograft groups ( $P = 0.863$ ). For the expression of *GDNF*, *PTN*, and *GAP43*, no significant differences were found between the groups ( $P = 0.849$ ,  $0.344$ ,  $0.557$ ).

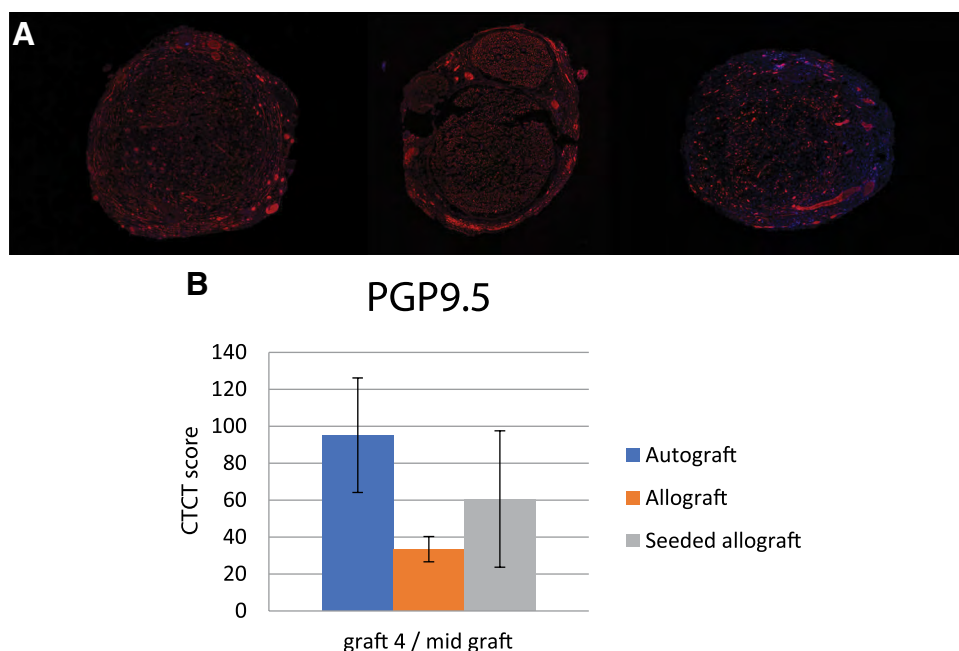


**Fig. 1.** A, PGP9.5 expression. Sections at the mid-graft stained with the (sensory) axonal marker PGP9.5 showed axons in the autograft, allograft and MSC seeded nerve allograft. Representative images are depicted with the double layer (DAPI). Magnification  $\times 10$ . Scale bar reflects 5 mm.  $n = 4$  animals per group. B, PGP9.5 staining intensity quantification. Quantitative analysis of PGP9.5 staining by calculating and comparing the average CTCT-score among groups. Images were analyzed without DAPI. No significant differences were found.  $n = 4$  animals per group.

Gene expression for the angiogenic molecule *VEGFA*, endothelial marker *CD31* and myelination factors *MPZ*, *PMP22*, and *MBP* is depicted in figure, Supplemental Digital Content 3b, <http://links.lww.com/PRSGO/>

**B270.** Analysis showed a significant 4.5-fold increase of *VEGFA* expression in seeded nerve allografts ( $P = 0.009$ ) and a significant 3.2-fold increase in autografts ( $P = 0.014$ ) when compared with the unseeded nerve

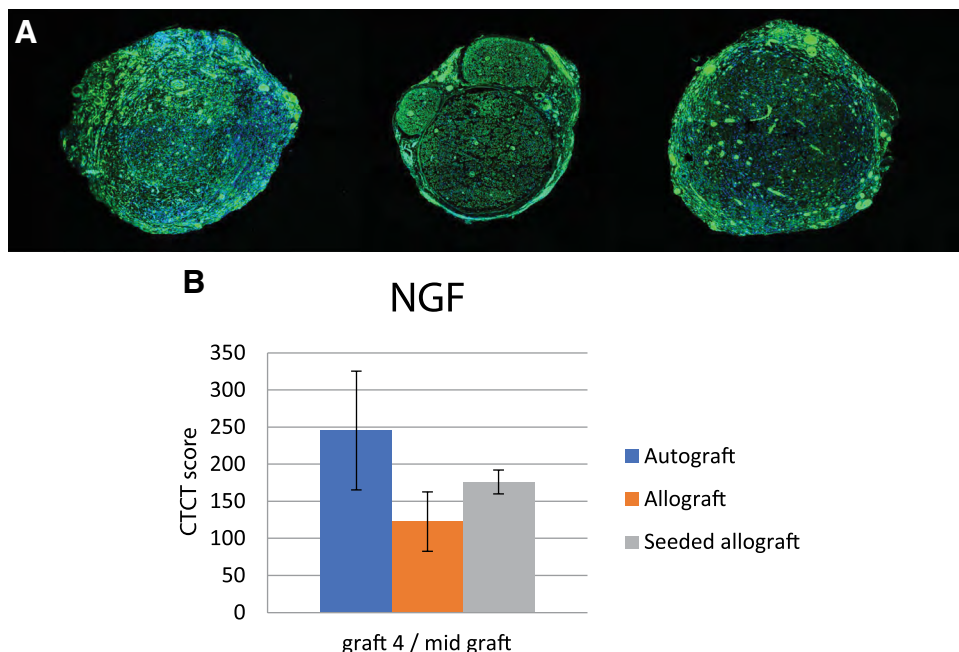


**Fig. 2.** A, NGF expression. Sections at the mid-graft stained for NGF showed presence of the marker in the autograft, allograft, and MSC seeded nerve allograft. Representative images are depicted with the double layer (DAPI). Magnification  $\times 10$ . Scale bar reflects 5 mm.  $n = 4$  animals per group. B, NGF staining intensity quantification. Quantitative analysis of NGF staining by calculating and comparing the average CTCT-score among groups. Images were analyzed without DAPI. A significant increase of NGF expression in the autograft and MSC seeded allograft was found when compared with the unseeded nerve allograft.  $n = 4$  animals per group ( $*P < 0.05$ ).



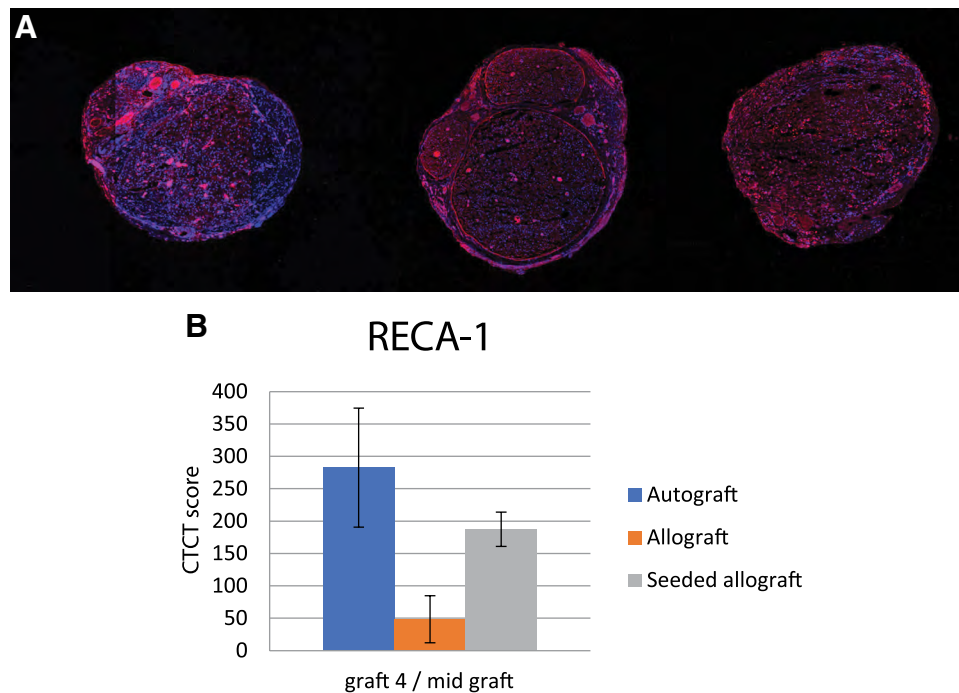


**Fig. 3.** A, RECA-1 expression. Sections at the mid-graft stained for endothelial marker RECA-1 showed presence of the marker in the autograft, allograft, and MSC seeded nerve allograft. Representative images are depicted with the double layer (DAPI). Magnification  $\times 10$ . Scale bar reflects 5 mm.  $n = 4$  animals per group. B, RECA-1 staining intensity quantification. Quantitative analysis of RECA-1 staining by calculating and comparing the average CTCF-score among groups. Images were analyzed without DAPI. A significant increase of RECA-1 expression in the autograft and MSC seeded allograft was found when compared with the unseeded nerve allograft.  $n = 4$  animals per group ( $*P < 0.05$ ).

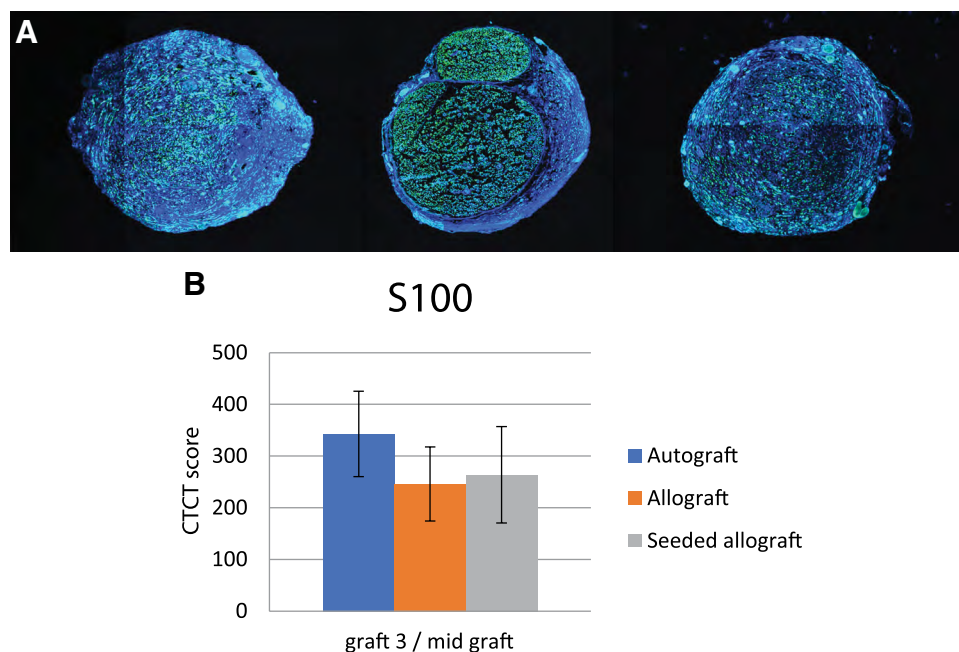


**Fig. 4.** A, S100 expression. Sections at the mid-graft stained for SC marker S100 showed presence of the marker in the autograft, allograft, and MSC seeded nerve allograft. Representative images are depicted with the double layer (DAPI). Magnification  $\times 10$ . Scale bar reflects 5 mm.  $n = 4$  animals per group. B, S100 staining intensity quantification. Quantitative analysis of S100 staining by calculating and comparing the average CTCF-score among groups. Images were analyzed without DAPI. No significant differences were found.  $n = 4$  animals per group.

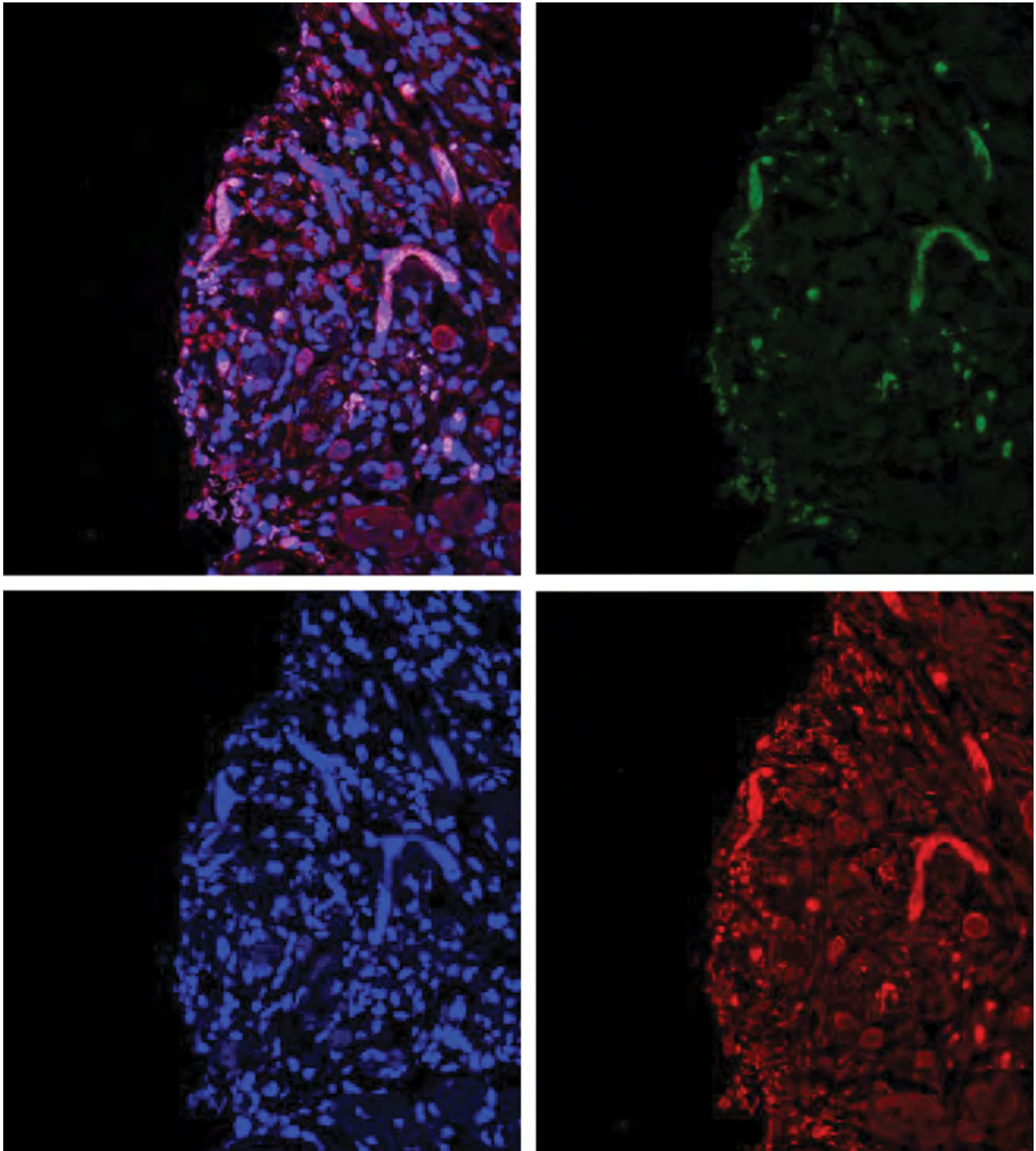


**Fig. 5.** Luciferase and S100 double stain. Sections at the mid-graft of MSC seeded nerve allografts have been stained for anti-Luciferase (red) and SC marker S100 (green). Cell nuclei were stained by DAPI (blue). Overlapping images are shown in the right column. Many Luciferase positive cells are negative for S100, indicating that the implanted cells did not differentiate into a SC phenotype. Magnification  $\times 20$ . Scale bar reflects 100  $\mu\text{m}$ .  $n = 4$  animals.

allografts. For *CD31*, an increasing trend (1.2-fold) was observed as well in the seeded allograft group; however, differences were not significant ( $P = 0.616$ ). Myelination markers *MPZ*, *PMP22*, and *MBP*, required for formation and maintenance of myelin, were all equally expressed.

ECM-related markers *COL1A1* and *COL3A1* were highly expressed in all groups and no significant differences were found. The *LAMB2* and *FBLN1* genes play a role in cell adhesion, differentiation, and migration. Expression was moderate in all groups and differences

were non-significant (see figure, Supplemental Digital Content 3c, <http://links.lww.com/PRSGO/B270>).<sup>24</sup>

Additional genes (see figure, Supplemental Digital Content 3d, <http://links.lww.com/PRSGO/B270>) were evaluated to map MSC characteristics including proliferation and apoptosis. A non-significant increase (2.2-fold) in *CASP3* in MSC seeded allografts when compared with the autograft and unseeded allograft was found. For *EGR1*, no significant differences were found. The *SOX2* gene mRNA level was significantly downregulated (0.3-fold,  $P = 0.006$ ) in MSC seeded allografts. No significant differences were found for *CCNB2* and *FABP4*.

### Immunohistochemical Staining

PGP9.5 was assessed to quantify the amount of newly formed (sensory) axons. The marker was present in all 3 groups and representative images are depicted in Fig. 1A. The CTCF score in the nerve autograft ( $95.2 \pm 30.9$ ) was increased when compared with the unseeded allograft ( $33.4 \pm 6.8$ ) and MSC seeded allograft ( $60.6 \pm 36.9$ ), respectively. The MSC seeded graft showed an increased expression but not significant when compared with the unseeded allograft (Fig. 1B).

NGF is critical in regeneration, survival, and maintenance of neurons and is expressed during early neural development.<sup>25</sup> NGF was relatively highly expressed in all 3 groups (Fig. 2A). Both the CTCF score of the nerve autograft ( $245.2 \pm 79.8$ ) and the MSC seeded allograft ( $175.9 \pm 16.1$ ) were significantly increased ( $P = 0.007$  and  $P = 0.018$ ) when compared with the unseeded allograft ( $122.6 \pm 40.1$ ). There were no significant differences between the autograft and seeded allograft (Fig. 2B).

RECA-1 is expressed in rat endothelial cells and was used to study angiogenesis.<sup>25</sup> RECA-1 was highly expressed in the autograft and MSC seeded allograft group (Fig. 3A). Both the CTCF score of the nerve autograft ( $282.6 \pm 91.9$ ) and the MSC seeded allograft ( $187.5 \pm 26.5$ ) were significantly increased ( $P = 0.007$  and  $P = 0.018$ ) when compared with the unseeded allograft ( $48.4 \pm 36.5$ ). There were no significant differences between the autograft and seeded allograft (Fig. 3B).

S100 was measured to assess the amount of SC-like cells. The marker was highly expressed in all groups and representative images are depicted in Fig. 4A. Quantification of the expression showed no significant differences between groups in CTCF score for the nerve autograft ( $342.8 \pm 82.6$ ), unseeded allograft ( $245.9 \pm 71.6$ ), and MSC seeded allograft ( $263.7 \pm 93.3$ ), respectively (Fig. 4B).

Luciferase-labeled MSCs were double stained for Luciferase and S100 to study MSC differentiation to SC-like cells. Luciferase-positive cells were detected in high abundance in the peripheral areas of the nerve graft, but only a few showed co-staining with S100. Many luciferase-positive cells were negative for S100, indicating that the implanted cells did not differentiate in large numbers into SC-like cells (Fig. 5).

## DISCUSSION

We report on early regenerative parameters following nerve repair by a decellularized nerve allograft pre-seeded

with adipose-derived MSCs and compare it to the unseeded allograft and autograft nerve.

NGF is important for the development and maintenance of the sympathetic and sensory nervous systems.<sup>11</sup> NGF gene-expression was significantly increased in autografts, which correlates with the increasing trend in NGF staining intensity. However, in seeded allografts, NGF staining intensity was significantly increased when compared with unseeded allografts, suggesting that MSC seeded nerve allografts support the regeneration of sensory nerves to a greater extent than unseeded nerve allografts. NGF is not expressed by motor neurons, is barely detectable in healthy sciatic nerves, and, following nerve injury, it shows a biphasic upregulation in the distal nerve stump during the first week of regeneration.<sup>11</sup> NGF mRNA decrease can be explained by either the motor origin of the nerve allografts, or the solitary 2-week time point. It is possible that in both allograft groups, levels were increased in the first week and were already normalized at week 2.

Both the *VEGFA*-gene and *CD31* are involved in angiogenesis and endothelial cell growth. *VEGFA* plays a role in wound healing, can promote neovascularization, and has a neurotrophic effect in enhancing the survival of SCs and protecting neurons from ischemic injury.<sup>26</sup> *VEGFA* molecule was significantly increased in seeded allografts and *CD31* showed the same increasing trend. This correlates with the significantly increased RECA-1 intensity in seeded nerve grafts; however, the intensity was also significantly increased in autografts. Previous studies have reported beneficial effects of VEGFA on vascularization, resulting in improved regeneration in acellular grafts.<sup>27</sup> Kingham et al<sup>28</sup> showed that in addition to acting directly on the nervous system, (differentiated) MSCs were able to boost vascularization at the area of nerve injury. Similar to our results, the authors showed an increased VEGFA secretion and RECA-1 staining intensity. Other studies have confirmed the correlation between increased vascularization and enhanced nerve regeneration within acellular conduits.<sup>29,30</sup>

*CASP3* was measured to assess the potential of seeded MSCs to mediate cell apoptosis. We hypothesized that MSCs would reduce apoptosis, but the increase in seeded allografts suggests that a portion of the cells go into apoptosis. We previously showed that implanted undifferentiated MSCs do not survive longer than 4 weeks and that the number of cells gradually diminishes over time.<sup>15</sup> Kingham et al<sup>28</sup> showed that *CASP3* levels were significantly reduced when nerve conduits were filled with stimulated cells, while unstimulated MSCs had no significant effect. This could suggest that differentiated cells survive longer than undifferentiated cells.

The *SOX2* gene is a key transcription factor in the regulation of pluripotency and neural differentiation. Cells expressing *SOX2* are capable of proliferating and producing differentiated neural cell types.<sup>31</sup> Transcription factor *SOX2* was significantly downregulated in seeded allografts, suggesting that after 2 weeks, seeded MSCs no longer proliferate and may have reached a differentiated state. MSCs may not have differentiated into SC-like cells



as there was no increase in myelination markers and only a moderate increase in S100 staining intensity. This is in line with previous reports that found no histological evidence of MSC transdifferentiation into SC-like cells within 14-days follow-up.<sup>32,33</sup> Others concluded that the therapeutic effect was maintained for several weeks after there were no significant quantities of viable cells and concluded that the regenerative effect of MSCs was mediated by an initial boost of released growth factors or by an indirect effect on endogenous SC activity.<sup>2,34</sup> In line with these results, Wang et al<sup>35</sup> detected only few S100 positive cells after implanting MSCs in an acellular nerve allograft.

The anti-luciferase and S100 double stain confirmed that implanted cells did not differentiate in large numbers into a SC phenotype. This is consistent with previous reports, concluding that adipose-derived MSCs do not differentiate into SCs but probably secrete some type of humoral factor or VEGFA that promotes the proliferation or migration of SCs.<sup>36</sup> Sowa et al<sup>37</sup> also concluded that undifferentiated implanted adipose-derived MSCs did not differentiate into SC but do promote peripheral nerve regeneration at the injured site.

*In vitro*, it has been shown that the cues of the ECM increased neurotrophic gene expression.<sup>24</sup> *In vivo*, undifferentiated cells may undergo differentiation in response to local stimuli. The hypoxic milieu of the wound might have triggered the MSCs to produce angiogenic molecules; which could be the underlying mechanism of MSCs restorative capacity. Wang et al<sup>38</sup> concluded that *in vivo* differentiation was safer, site-dependent, and entirely under the control of signals from the endogenous microenvironment.

Undifferentiated MSCs can potentially differentiate into unwanted cell types or form teratomas; however, this risk is very low. Because undifferentiated MSCs only develop into cells of mesodermal lineages, while the composition of teratoma requires all 3 germ cell layers.<sup>39</sup> Klein et al<sup>10</sup> reported there is controversy regarding whether this risk of malignant transformation is evident for adipose-derived MSCs and reported no tumor formations in their study. Nonetheless, for future clinical implementation this potential risk has to be investigated.

Strengths of this study include the use of a non-damaging cell seeding technique and a design that mimics the human situation with major histocompatibility complex mismatched allograft donors and recipients.

We recognize the limitations of this study. Successful axonal regeneration depends on a dynamic balance between growth factors and analysis of multiple time points would provide more insight. No functional measurements were performed because 2 weeks is too early for any motor reinnervation to occur. Future studies should focus on the growth factor expression at multiple time-points and should determine if the initially improved regenerative response of MSCs enhanced decellularized nerve allografts results in enhanced functional recovery.

## CONCLUSIONS

We aimed to evaluate the molecular mechanisms underlying nerve repair by a decellularized nerve allograft

seeded with undifferentiated MSCs. We confirmed that MSCs contribute to the secretion of trophic factors, resulting in a beneficial effect of the MSCs on angiogenesis. Implanted MSCs did not show evidence of differentiation into SC-like cells.

**Nadia Rbia, MD**

Department of Plastic, Reconstructive and Hand surgery  
Erasmus MC, University Medical Center  
Room Ee 1591  
Postal Box 2040, 300 CA Rotterdam  
The Netherlands  
E-mail: n.rbia@erasmusmc.nl

## REFERENCES

1. Rbia N, Shin AY. The role of nerve graft substitutes in motor and mixed motor/sensory peripheral nerve injuries. *J Hand Surg Am.* 2017;42:367–377.
2. Jiang L, Jones S, Jia X. Stem cell transplantation for peripheral nerve regeneration: current options and opportunities. *Int J Mol Sci.* 2017;18:94.
3. di Summa PG, Kalbermatten DF, Pralong E, et al. Long-term *in vivo* regeneration of peripheral nerves through bioengineered nerve grafts. *Neuroscience.* 2011;181:278–291.
4. Rodríguez FJ, Verdú E, Ceballos D, et al. Nerve guides seeded with autologous Schwann cells improve nerve regeneration. *Exp Neurol.* 2000;161:571–584.
5. Walsh S, Midha R. Practical considerations concerning the use of stem cells for peripheral nerve repair. *Neurosurg Focus.* 2009;26:E2.
6. Wang Y, Zhao Z, Ren Z, et al. Recellularized nerve allografts with differentiated mesenchymal stem cells promote peripheral nerve regeneration. *Neurosci Lett.* 2012;514:96–101.
7. Sun XH, Che YQ, Tong XJ, et al. Improving nerve regeneration of acellular nerve allografts seeded with scs bridging the sciatic nerve defects of rat. *Cell Mol Neurobiol.* 2009;29:347–353.
8. Jesuraj NJ, Santosa KB, Macewan MR, et al. Schwann cells seeded in acellular nerve grafts improve functional recovery. *Muscle Nerve.* 2014;49:267–276.
9. Georgiou M, Golding JP, Loughlin AJ, et al. Engineered neural tissue with aligned, differentiated adipose-derived stem cells promotes peripheral nerve regeneration across a critical sized defect in rat sciatic nerve. *Biomaterials.* 2015;37:242–251.
10. Klein SM, Vykoukal J, Li DP, et al. Peripheral motor and sensory nerve conduction following transplantation of undifferentiated autologous adipose tissue-derived stem cells in a biodegradable U.S. Food and drug administration-approved nerve conduit. *Plast Reconstr Surg.* 2016;138:132–139.
11. Boyd JG, Gordon T. Neurotrophic factors and their receptors in axonal regeneration and functional recovery after peripheral nerve injury. *Mol Neurobiol.* 2003;27:277–324.
12. Zhao Z, Wang Y, Peng J, et al. Improvement in nerve regeneration through a decellularized nerve graft by supplementation with bone marrow stromal cells in fibrin. *Cell Transplant.* 2014;23:97–110.
13. Hudson TW, Liu SY, Schmidt CE. Engineering an improved acellular nerve graft via optimized chemical processing. *Tissue Eng.* 2004;10:1346–1358.
14. Kingham PJ, Kalbermatten DF, Mahay D, et al. Adipose-derived stem cells differentiate into a Schwann cell phenotype and promote neurite outgrowth *in vitro*. *Exp Neurol.* 2007;207:267–274.
15. Rbia N, Bulstra LF, Thaler R, et al. *In vivo* survival of mesenchymal stromal cell-enhanced decellularized nerve grafts for segmental peripheral nerve reconstruction. *J Hand Surg Am.* 2019;44:514.e1–514.e11.



16. Hundepool CA, Nijhuis TH, Kotsougiani D, et al. Optimizing decellularization techniques to create a new nerve allograft: an *in vitro* study using rodent nerve segments. *Neurosurg Focus*. 2017;42:E4.
17. Rbia N, Bulstra LF, Bishop AT, et al. A simple dynamic strategy to deliver stem cells to decellularized nerve allografts. *Plast Reconstr Surg*. 2018;142:402–413.
18. Hundepool CA, Bulstra LF, Kotsougiani D, et al. Comparable functional motor outcomes after repair of peripheral nerve injury with an elastase-processed allograft in a rat sciatic nerve model. *Microsurgery*. 2018;38:772–779.
19. Höke A, Redett R, Hameed H, et al. Schwann cells express motor and sensory phenotypes that regulate axon regeneration. *J Neurosci*. 2006;26:9646–9655.
20. Jesuraj NJ, Nguyen PK, Wood MD, et al. Differential gene expression in motor and sensory Schwann cells in the rat femoral nerve. *J Neurosci Res*. 2012;90:96–104.
21. Kingham PJ, Reid AJ, Wiberg M. Adipose-derived stem cells for nerve repair: hype or reality? *Cells Tissues Organs*. 2014;200:23–30.
22. Dudakovic A, Camilleri E, Riester SM, et al. High-resolution molecular validation of self-renewal and spontaneous differentiation in clinical-grade adipose-tissue derived human mesenchymal stem cells. *J Cell Biochem*. 2014;115:1816–1828.
23. Jensen EC. Quantitative analysis of histological staining and fluorescence using imagej. *Anat Rec (Hoboken)*. 2013;296:378–381.
24. di Summa PG, Kalbermatten DF, Raffoul W, et al. Extracellular matrix molecules enhance the neurotrophic effect of Schwann cell-like differentiated adipose-derived stem cells and increase cell survival under stress conditions. *Tissue Eng Part A*. 2013;19:368–379.
25. Kaplan DR, Miller FD. Neurotrophin signal transduction in the nervous system. *Curr Opin Neurobiol*. 2000;10:381–391.
26. Fan L, Yu Z, Li J, et al. Schwann-like cells seeded in acellular nerve grafts improve nerve regeneration. *BMC Musculoskelet Disord*. 2014;15:165.
27. Hoyng SA, De Winter F, Gnani S, et al. A comparative morphological, electrophysiological and functional analysis of axon regeneration through peripheral nerve autografts genetically modified to overexpress BDNF, CNTF, GDNF, NGF, NT3 or VEGF. *Exp Neurol*. 2014;261:578–593.
28. Kingham PJ, Kolar MK, Novikova LN, et al. Stimulating the neurotrophic and angiogenic properties of human adipose-derived stem cells enhances nerve repair. *Stem Cells Dev*. 2014;23:741–754.
29. Hobson MI, Green CJ, Terenghi G. VEGF enhances intraneural angiogenesis and improves nerve regeneration after axotomy. *J Anat*. 2000;197(Pt 4):591–605.
30. Sowa Y, Imura T, Numajiri T, et al. Adipose-derived stem cells produce factors enhancing peripheral nerve regeneration: influence of age and anatomic site of origin. *Stem Cells Dev*. 2012;21:1852–1862.
31. Suh H, Consiglio A, Ray J, et al. *In vivo* fate analysis reveals the multipotent and self-renewal capacities of sox2+ neural stem cells in the adult hippocampus. *Cell Stem Cell*. 2007;1:515–528.
32. Shen J, Duan XH, Cheng LN, et al. *In vivo* MR imaging tracking of transplanted mesenchymal stem cells in a rabbit model of acute peripheral nerve traction injury. *J Magn Reson Imaging*. 2010;32:1076–1085.
33. Santiago LY, Clavijo-Alvarez J, Brayfield C, et al. Delivery of adipose-derived precursor cells for peripheral nerve repair. *Cell Transplant*. 2009;18:145–158.
34. Kappos EA, Engels PE, Tremp M, et al. Peripheral nerve repair: multimodal comparison of the long-term regenerative potential of adipose tissue-derived cells in a biodegradable conduit. *Stem Cells Dev*. 2015;24:2127–2141.
35. Wang Y, Jia H, Li WY, et al. Synergistic effects of bone mesenchymal stem cells and chondroitinase ABC on nerve regeneration after acellular nerve allograft in rats. *Cell Mol Neurobiol*. 2012;32:361–371.
36. Suganuma S, Tada K, Hayashi K, et al. Uncultured adipose-derived regenerative cells promote peripheral nerve regeneration. *J Orthop Sci*. 2013;18:145–151.
37. Sowa Y, Kishida T, Imura T, et al. Adipose-derived stem cells promote peripheral nerve regeneration *in vivo* without differentiation into schwann-like lineage. *Plast Reconstr Surg*. 2016;137:318e–330e.
38. Wang D, Liu XL, Zhu JK, et al. Bridging small-gap peripheral nerve defects using acellular nerve allograft implanted with autologous bone marrow stromal cells in primates. *Brain Res*. 2008;1188:44–53.
39. Zhang R, Rosen JM. The role of undifferentiated adipose-derived stem cells in peripheral nerve repair. *Neural Regen Res*. 2018;13:757–763.